Sustainable Energy & Fuels

ROYAL SOCIETY OF CHEMISTRY

PAPER

View Article Online
View Journal | View Issue

Cite this: *Sustainable Energy Fuels*, 2023, 7, 398

A single-cell system of flow electrode capacitive mixing (F-CapMix) with a cross chamber for continuous energy production

Zhi Zou, *[a] Shuo Meng,[b] Xiaolei Bian[a] and Longcheng Liu*[ab]

The generation of electricity from salinity difference energy between seawater and freshwater through a Capacitive Mixing (CapMix) system with solid electrodes was limited by intermittent energy production. In this study, a single-cell CapMix system using flow-electrode (F-CapMix) with a cross-chamber configuration was examined to produce electricity continuously from simulated seawater and freshwater. The effects of the flow-electrode electrolyte concentration, activated carbon loading, amounts of carbon black, and connected external resistance on the system performance were investigated. The results suggest that the system performance can be enhanced by increasing the activated carbon loading and carbon black amounts. Furthermore, to achieve the maximum power density of the system, the external resistance should be matched to the internal resistance. The maximum power density of the presented single-cell F-CapMix system was 74.3 mW m^{-2}, which was comparable to those of previous CapMix and F-CapMix systems. In addition, this study also reveals that using only carbon black as the flow electrode is capable of producing electricity continuously for long-term operation. In summary, these results indicate the potential of F-CapMix and provide developing directions for further optimization.

Received 8th November 2022
Accepted 30th November 2022

DOI: 10.1039/d2se01546c

rsc.li/sustainable-energy

1 Introduction

With continuous population growth and economic development, the global demand for accessible energy is growing. According to the BP Statistical Review of World Energy 2021, non-renewable energy sources, *i.e.*, oil, natural gas, and coal, are the most used energy sources in world energy consumption, accounting for more than 80 percent.[1] However, these non-renewable energy sources suffer from limited resources as well as environmental pollution from the production and transportation process.[2] In contrast, renewable energy is regarded as a clean, sustainable, and affordable energy source.[3] Based on these merits, the production and use of renewable energy have been strongly increasing in recent years. It has accounted for around 60% of the growth in global power generation from 2016 to 2020.[1] Among the various renewable energy sources, salinity gradient energy (SGE) that utilizes the Gibbs free energy from the mixing of two solutions with different concentrations, *i.e.*, seawater and freshwater, is an overlooked energy source but has great potential.[4] Theoretically, around 0.81 kW h energy could be extracted from mixing 1 m^3 of freshwater with the same amount of seawater, which is equivalent to the energy released from water falling over a dam of 270 m.[5–7] It has been estimated that the practically extractable SGE around the world is about 625 TW h per year, which is equivalent to 3% of global electricity consumption.[8]

Given the tremendous potential of SGE worldwide, many technologies have been proposed and developed to harvest this sustainable energy source. To date, the leading methods of extracting SGE include pressure retarded osmosis (PRO),[9] reverse electrodialysis (RED),[10] and capacitive mixing (CapMix).[11–13] PRO utilizes the osmotic pressure difference across a semipermeable membrane to drive the solution flow from the dilute water compartment to the concentrated water compartment. The expanding solution volume propels a hydroturbine to generate energy.[6,9] In RED, the dilute water and the concentrated water alternatively flow through the compartments divided by a stack of cation and anion-exchange membranes, and the transportation of ions through the membranes leads to an electric current between the cathode and anode.[2,10,14] In CapMix, the electrodes are periodically charging and discharging in the seawater and fresh water, resulting in a cyclically changing electric potential difference to transfer the chemical potential in the salinity difference to practical work.[4,11–13] Among them, CapMix is the latest and is the focus of the present study.

In principle, three CapMix techniques have been proposed depending on the transportation pattern of ions into the

[a]*Department of Chemical Engineering, School of Engineering Sciences in Chemistry, Biotechnology and Health, KTH Royal Institute of Technology, 10044 Stockholm, Sweden. E-mail: lliu@ket.kth.se*

[b]*School of Nuclear Science and Technology, University of South China, 421001, Hengyang, China*

electrodes from the bulk solution.[15,16] The first one is capacitive energy extraction based on the capacitive double-layer expansion (CDLE), which is a membranes-free technology that utilizes an external power source to accomplish the energy extraction process.[11] The second one is capacitive energy extraction based on the capacitive Donnan potential (CDP), in which the electrodes are covered by ion-exchange membranes (IEMs) that develop a Donnan potential to extract the SGE instead of using an external power source.[12] The last one is a soft electrode (SE), in which the electrodes are coated with negatively or positively charged polyelectrolyte layers to generate a potential difference to harvest the SGE. No IEMs and external power sources are used in the SE.[13] To date, many studies on CapMix have been conducted to enhance the system performance, including the development and modification of electrode materials;[17–22] design and application of innovative cell configuration, *i.e.*, using a wire geometry cell[23] and stacking of cells;[24] optimization of the operating parameters (*e.g.*, temperature[25,26] and the flow rate of the solution[27]); the combination of these techniques (*e.g.*, CDP with CDLE,[28] and CDLE with SE[16]) In addition to the extensive experimental studies, corresponding theoretical modeling studies were also performed to understand the process behavior.[29–31] However, the use of solid electrodes in CapMix makes it produce energy in an intermittent way, *i.e.*, the ions are first adsorbed into the electrodes by external power (*e.g.*, voltage or current) or membrane potential until the electrodes are saturated with ions, and the adsorbed ions are then released from the electrodes. This discontinuous energy supply is insufficient to meet basic power requirements for practical applications.[32,33]

Recently, an innovative design using an activated carbon suspension as the electrode was introduced in the capacitive technique to overcome the finite ion storage capacity of solid electrodes.[34] This flowable electrode's design was first applied in desalination (FCDI)[34–36] and was then applied in the CapMix (F-CapMix) field for energy production.[37,38] The research on F-CapMix is still at the initial stage, and limited studies have been reported so far.[15,21,33,39,40] Theoretically, this F-CapMix technique is capable of producing energy continuously by unintermittently supplying fresh flow electrode (FE). However, this leads to a massive waste of activated carbon. For a practical F-CapMix system, the FE was recirculated within the system, and the activated carbon (AC) in the flow electrode (FE) slurry will be saturated without regeneration. It has been reported that the energy production and regeneration of the FE can be achieved simultaneously through a system with four cells connected in series.[37] However, a system with extra cells will make the system more complex to operate. Therefore, designing a continuous system with only one cell performing energy production and FE regeneration at the same time is highly desirable. Recently, Liu *et al.*[33] developed a single-cell system with a graphite brush and graphite plates (without caved channels) as current collectors to generate electricity continuously. While Liu *et al.*[33] took the first step and developed a one-cell system suggesting that the system performance can be significantly enhanced by using a graphite brush as a current collector compared to flat graphite plates (without caved channels), for a large cell, the use of flat graphite plates (without caved channels) might lead to a great dead-zone of the FE due to the great viscosity of the FE. Here in this study, we use a more application-oriented method based on the utilization of graphite plates with caved channels as current collectors, which is now widely used in FCDI[41,42] and F-CapMix systems,[15,39] to produce electricity from salinity gradient energy. But using graphite plates with caved channels in a single cell F-CapMix system with a cross chamber design for continuous energy production, to the best of our knowledge, has not yet been detailed investigated.

It is generally believed that all techniques based on such a flowable electrode design depend heavily on the adsorption capacity of electrodes. Therefore, activated carbon (AC) with a high surface area is widely used in FCDI and F-CapMix systems.[15,43,44] However, due to the poor electronic conductivity of AC suspension, the FE was made of a high AC loading or the mixture of AC with additional small amounts of conductive additives, such as carbon black (CB) with high conductivity, to elevate the electronic conductivity of the FE. And recently, it has been proved that using only carbon black with high conductivity and a low specific surface area as electrodes for desalination in FCDI can outperform microporous AC-based electrodes.[45] To the best of our knowledge, there is low research on the F-CapMix system using only CB for extracting SGE, which will be addressed in the present study.

In the present study, we experimentally examined the feasibility of simultaneous energy extraction and regeneration of the FE in a single-cell F-CapMix system with a cross-chamber design. The system performance was investigated under different conditions, including the electrolyte concentration in the FE, carbon weight percentage or carbon loading, additional carbon black amounts, and external resistance. In addition, the performance of the F-CapMix system using CB solely as the electrodes was investigated.

2 Materials and methods

2.1 Materials

The sodium chloride (NaCl) used in the present study was analytical reagent grade and was purchased from Aladdin Industrial Co., Ltd. (Shanghai, China). The activated carbon used in the present study was YP-50F (Kuraray Chemical Company, Tokyo, Japan). Three different carbon black (CB) samples were applied as conductive additives and electrodes in this study: (1) CB (Ketjenblack ECP600JD, Lion Corporation, Tokyo, Japan), (2) CB2 (Ketjenblack ECP, Lion Corporation, Tokyo, Japan) and CB3 (DENKA acetylene black, Denka Company Limited, Tokyo, Japan). A synthetic 500 mM NaCl high concentration (HC) and a 20 mM NaCl low concentration (LC) water were used to simulate the seawater and freshwater, respectively.

2.2 Experimental setup and operation

The configuration of the F-CapMix cell used in this study is shown in Fig. 1. The F-CapMix cell was assembled with the following components: two acrylic-made plates (150 mm ×

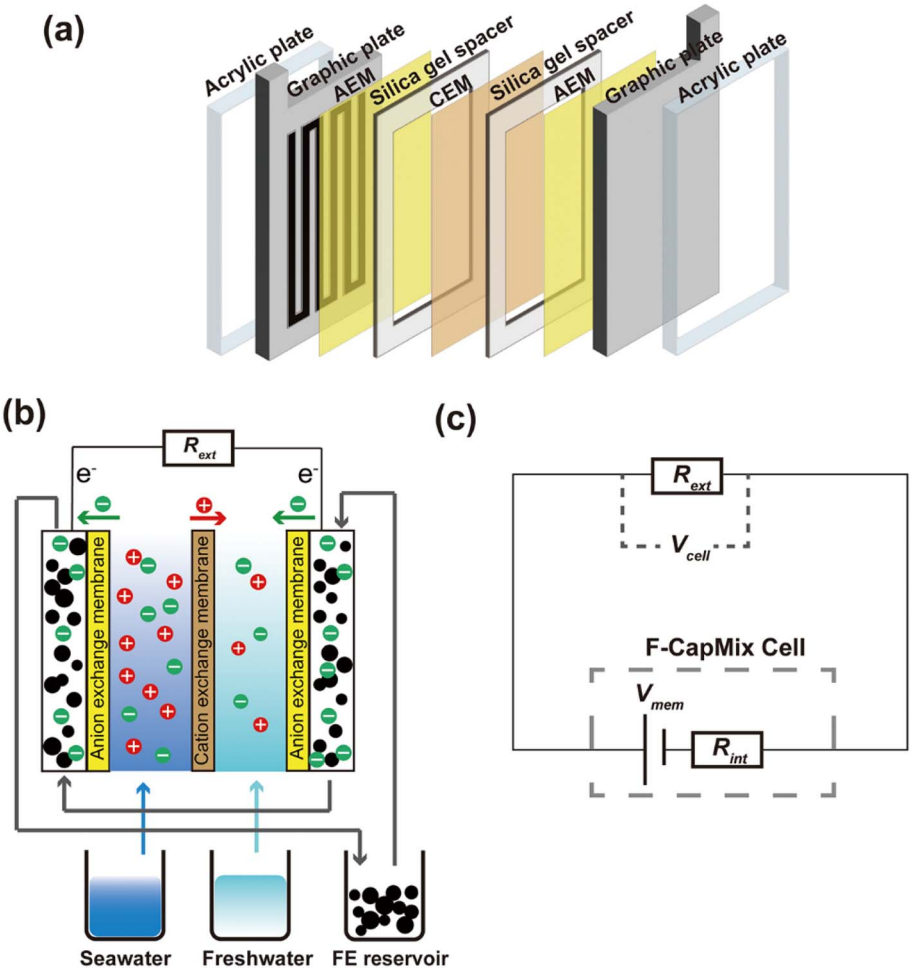

Fig. 1 Schematic of (a) the main components of an F-CapMix cell, (b) experimental setup, and (c) F-CapMix circuit.

80 mm × 10 mm) as the supporting plates, two graphitic-made plates (150 mm × 80 mm × 7 mm) as the current collectors, two silicon gaskets (thickness: 0.5 mm) with hollow space (110 mm × 42 mm) as the flow channel of the feedwater (FW) of seawater and freshwater, two anion-exchange membranes (AEM, HMTECH—E18230, HUAMOTECH, China), and a cation-exchange membrane (CEM, HMTECH—E17270, HUAMOTECH, China) were placed on the joints between the silicon gaskets and graphitic plates. Each graphitic plate was engraved with flow channels (cross-section: 2 mm × 2 mm, length: 11 cm, and the number of paths: 11) on the surface for FE slurry flowing through. To ensure the uniform distribution of FW in the spacer, five nylon sheets (thickness: 0.1 mm and 100 mesh for each) were placed in the hollow part of the silicon gasket. All the components were fastened together with an M5 screw. The FE slurry and FW were pumped into the cell by two peristaltic pumps (L100-1S-1, Longer Precision Pump Co., Ltd., China). During the operation, the FE slurry was continuously recirculated in the cell, while the FW was pumped into the cell in a single-pass mode. The cell voltage of the F-CapMix system V_{cell} was recorded by using an electrochemical workstation (CS3104, Wuhan Corrtest Instrument Corp, China).

There was no external power used in this system. The salinity gradient between the membrane generates an electrochemical potential that is known as the Nernst potential or the Donnan potential V_D, as:

$$V_D = \frac{\alpha}{z}\frac{RT}{F}\ln\left(\frac{c_{HC}}{c_{LC}}\right) \quad (1)$$

where α is the permselectivity of the membrane, z is the ion valence (*e.g.*, $z = 1$ for NaCl), R is the gas constant (8.314 J (mol^{-1} K^{-1})), T is the absolute temperature (298 K), F is the Faraday constant (96 485 C mol^{-1}), c is the mole concentration (mol m^{-3}), and the subscripts HC and LC represent water with high concentration and low concentration, respectively.

The sum of the Nernst potential across the membranes in a cell represents the membrane potential V_{mem}, which is also the cell's open circuit voltage.

To exploit the extracted salinity gradient energy from the CapMix system, it is necessary to connect the cell to a device, which was usually replaced by an external resistor in previous research.[27,37,46] The performance of the system can be quantified by power density, which can be calculated from the cell voltage V_{cell}, external resistance R_{ext}, and projection area of the

membrane A_m on the hollow part of the gasket (46.2 cm^2 in the present study), as:

$$P = \frac{{V_{cell}}^2}{R_{ext} A_m} \quad (2)$$

The overall performance is represented by the average power density of the experimental duration.

For an F-CapMix system, the cell is not ideally conductive but with some internal resistance that impedes the current in the circuit. In this way, an F-CapMix system can be represented as a power source V_{mem} that is in series with its internal resistance R_{int} and the external resistance R_{ext}, as shown in Fig. 1c. The internal resistance R_{int} can be roughly calculated from the membrane potential V_{mem}, the value of external load R_{ext}, and the cell voltage V_{cell}, as

$$R_{int} = \frac{V_{mem} R_{ext}}{V_{cell}} - R_{ext} \quad (3)$$

In this study, a series of experiments were performed to evaluate the effects of different experimental parameters (contents of AC and CB, and external resistance value R_{ext}) on the energy production of F-CapMix. The detailed experimental scheme is listed in Table 1. The FE slurry suspension was prepared by mixing different amounts of AC or CB materials with an 80 mL solution with different NaCl concentrations. The prepared FE slurry was continuously stirred overnight to wet AC/CB powders thoroughly. All experiments were conducted at room temperature (25 °C) in triplicate.

3 Results and discussion

3.1 Effect of FE concentration

The results obtained in a previous study using a four-cell F-CapMix revealed that the performance is dependent on the electrolyte concentration difference between FE and FW.[37] In this study, the effect of FE concentration on the performance of the cross-chamber F-CapMix system was investigated at three FE concentrations: 140, 260, and 380 mM, while the external resistance was fixed at 5 Ω. As can be seen in Fig. 2a, three experimental cases gave similar OCV results, at ~128 mV. After the circuit was connected with an external resistance, the cell voltage dropped from the OCV to a lower value (~16 mV) and then remained stable during the period of 10 hours of experimental operation for the three experimental groups with different FE concentrations (Fig. 2b). These stable cell voltages resulted in a stable power density during the operation (Fig. 2c). In the triplicated experiments of 10 hours' operation, similar performance was found for different FE concentrations (Fig. 2d). The stable voltage and power densities during the process proved the feasibility of this two-chamber F-CapMix system, indicating that the movement of ions reaches dynamic equilibrium conditions, *i.e.*, the number of ions transferred from FW into the FE on one side of the cell was equal to the number of ions released from the other side of the cell into FW. As a result, this system simultaneously realized the power production and regeneration of the FE within one cell unit, which is an improvement to the traditional F-CapMix system, whereas the regeneration of the FE requires an additional cell to accomplish.

Note that the similar OCVs of the present two-chamber F-CapMix system under the three different FE concentrations were not consistent with a prior reported F-CapMix system,[37] in which the OCVs were dependent on the FE concentrations. The reason for the difference can be attributed to the different cell configurations. For the prior F-CapMix system, there is only one FW chamber in the cell, and the OCV was the sum of the Nernst potential across the two membranes (one AEM and one CEM) that can be calculated from eqn (1), as $V_{mem}^{1c} = \left(\frac{\alpha_{CEM}}{z_+} + \frac{\alpha_{AEM}}{z_-}\right) \frac{RT}{F} \ln\left(\frac{c_{spacer}}{c_{FE}}\right)$. When the electrolyte concentration in the spacer c_{spacer} was fixed (*e.g.*, c_{spacer} = HC or LC), different FE electrolyte concentrations led to different OCVs. Meanwhile for the present two-chamber F-CapMix system, the OCV was the sum of the Nernst potential across the three membranes (two AEMs and one CEM) that can be represented as $V_{mem}^{2c} = \left(\frac{\alpha_{CEM}}{z_+} + \frac{\alpha_{AEM}}{z_-}\right) \frac{RT}{F} \ln\left(\frac{c_{spacer}^{HC}}{c_{spacer}^{LC}}\right)$. As a result, the OCV of this two-chamber F-CapMix system was only dependent on the concentration difference between the HC and LC. And the identical OCVs also explain the similar performance of this two-chamber F-CapMix system under different NaCl concentrations (Fig. 2d). Since the performance of this two-chamber F-CapMix system is independent of the NaCl concentration, we only used one NaCl concentration (260 mM) to perform the subsequent experiments.

Table 1 Experimental scheme for the F-CapMix system in the present study

NaCl concentration (mM)	Electrode content	External resistance (Ω)
140/260/380	5% AC	5
260	2.5%/5%/7.5%/10% AC	5
260	0.25% CB + 4.75% AC	5
260	0.5% CB + 4.5% AC	5
260	0.5% CB2 + 4.5% AC	5
260	0.5% CB3 + 4.5% AC	5
260	0.75% CB + 4.25% AC	5
260	1.0% CB + 4.0% AC	5
260	0.5%/1.0%/1.5% CB	5
260	0.5%/1.0%/1.5% CB2	5
260	0.5%/1.0%/1.5% CB3	5
260	5% AC	1/5/20/50/100

3.2 Effect of carbon loading on the system performance

The activated carbon (AC) in the FE plays an important role in conducting the electric charges and electrons in the F-CapMix system.[47] For analyzing the relationship between the power production of the present cross-chamber F-CapMix system and carbon loading in FE, experiments were conducted at four different carbon loadings: 2.5, 5.0, 7.5, and 10 wt%. As shown in Fig. 3a, a relatively steady cell voltage V_{cell} was found for all the

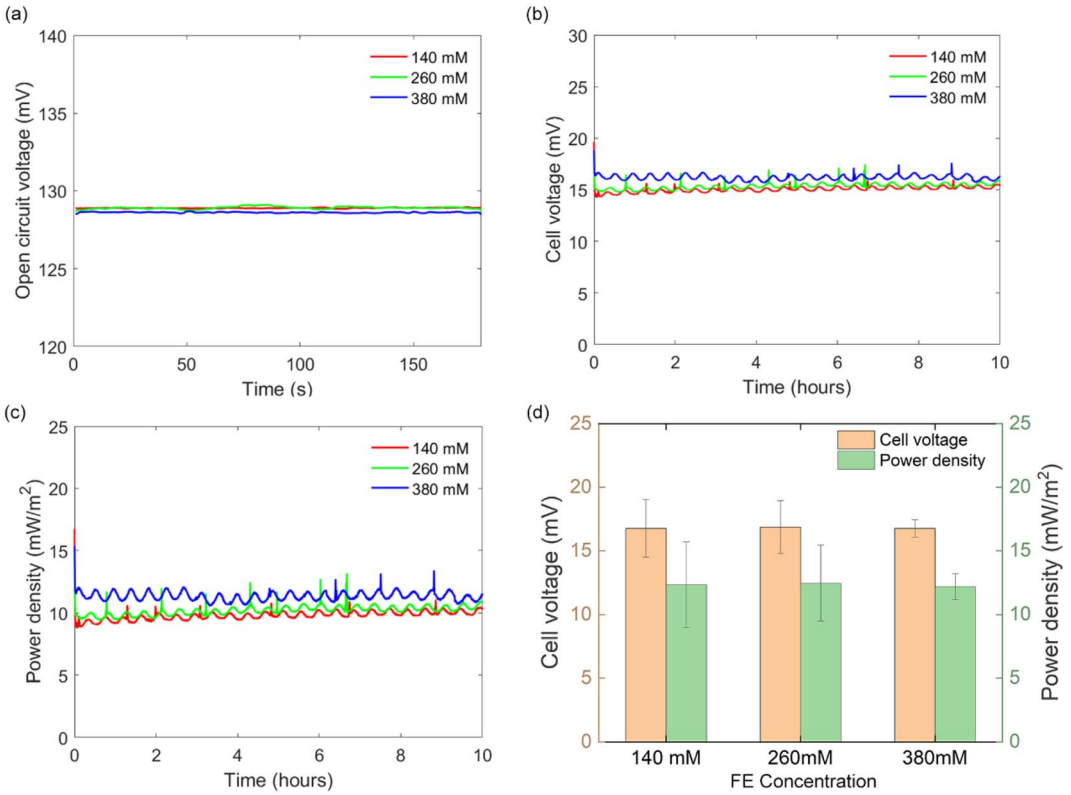

Fig. 2 Plot of (a) the open circuit voltage, (b) the cell voltage, and (c) the power density during the experiments. (d) The average cell voltage and the average power density at different FE concentrations, and the error bars denote the standard deviation for the triplicate experiments.

experimental cases, proving again that this F-CapMix successfully realized the energy production continuously for long-term operation. Meanwhile, V_{cell} was proportional to the carbon loading, increased by around 3-fold as the carbon loading increased from 2.5 to 10 wt%. The increased V_{cell} resulted in an enhanced power density P at a larger carbon loading as well (Fig. 3b). The power density increased from 5.5 to 46.1 mW m^{-2}, when the carbon loading increased from 2.5 to 10 wt%. These power densities are comparable to the power densities obtained with solid electrodes[11,12] as well as flow electrode systems of single[38] and multiple[37] reactor configurations. But the FE was continuously regenerated within the proposed single-cell F-CapMix system with a cross-chamber configuration, which greatly simplifies the cell configuration compared to the multiple-reactor configuration.[37]

The greater V_{cell} and P of the cross-chamber F-CapMix system at a higher carbon loading are consistent with those in a previous study.[37] The enhanced performance might be explained by the decreased internal resistance of the cell at a higher carbon loading. The internal resistance R_{int} can be calculated by using eqn (3), where V_{mem} is dependent on the electrolyte concentration of LC and HC, which was unchanged in the experiments (V_{mem} = ~129 mV), and R_{ext} (5 Ω) was unchanged for different carbon loadings as well. As a result, the higher V_{cell} at a higher carbon loading can only be attributed to the decrease of R_{int}. As shown in Fig. 4, R_{int} was decreased by 260% as the carbon loading increased from 2.5 to 10 wt%. In general, R_{int} consists of the setup resistance, the electronic resistance of flow electrodes, and the contact resistance between the electrode particles and the current collector.[36] It has been previously reported that increasing the carbon loading from 5 to 20 wt% in FE could significantly reduce both electronic and ionic resistance in the FE.[36] The reduced electronic resistance might be attributed to the larger average size of the percolating cluster of AC in the FE formed at a higher carbon loading, which facilitates the electron transport.[48,49] As a result, the charge and electron transportation within the FE was improved, and hence the performance was enhanced at a higher carbon loading.[38,50] Although the system performance can be enhanced by increasing the carbon loading in the FE, excessive AC amounts in the FE could increase the viscosity of the FE slurry and lead to the blockage of the FE channel and finally interrupt the experiments.[50] The blockage problem has been reported previously,[36,49] and the reason can be attributed to the hydrophobicity of AC and CB. In our study, the maximum carbon loading of the FE slurry that would not cause the clogging of the FE channel was 10 wt%, which is lower than the previously reported max carbon loading (*e.g.*, 20 to 35%).[35,50,51] The reason might be attributed to the different cell configurations (*e.g.*, the size of the FE channel and silicon tubes for the transportation of the FE) and the rheological properties of the utilized FE materials. Future work can focus on reducing the viscosity of FE slurry, *e.g.*, modifying the surface of AC materials through emulsion polymerization[50] or oxidative methods[52] to reduce its hydrophobicity.

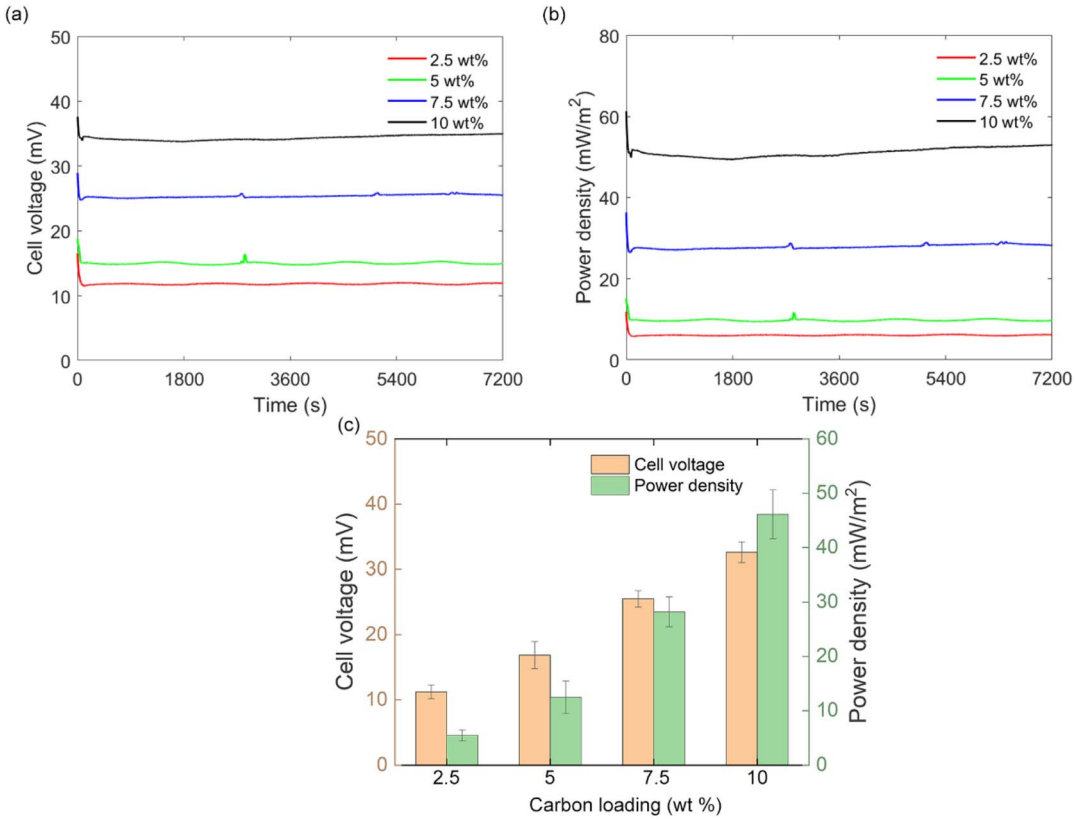

Fig. 3 Plot of (a) the cell voltage and (b) the power density during the experiments of different carbon loadings. (c) The average cell voltage and the average power density at different carbon loadings, and the error bars denote the standard deviation for the triplicate experiments.

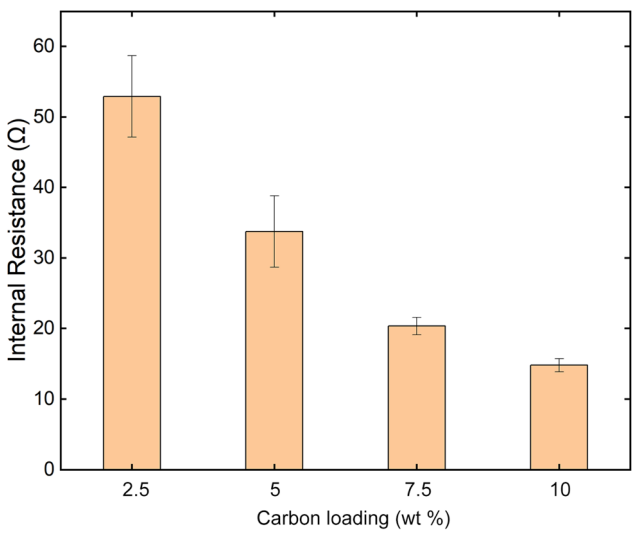

Fig. 4 Plot of the system's internal resistance R_{int} at different carbon loadings.

3.3 Effect of carbon black on the system performance

The above results suggested that the system performance of the F-CapMix system can be improved by increasing the carbon loading in the FE due to the reduction in the resistance of the FE. Other than increasing the carbon loading, the resistance of the FE can also be reduced by adding additional carbon black in the FE slurry.[35,53] To investigate the effects of CB amounts on the system performance, experiments were performed at five different CB amounts: 0.25, 0.5, 0.75, and 1.0 wt%, under a fixed total electrode (including AC and CB) loading of 5 wt%. As is expected, the cell voltage at different CB amounts was stable during the experiments. The performance of the system was increased with the additional amounts of CB (Fig. 5). The maximum average power density was found for the case of 4.0 wt% AC with 1.0 wt% additional CB amounts, at around 74.3 mW m^{-2}, which is around 6-fold the average power density of the case without additional CB.

The results in Fig. 5 proved that the system performance of F-CapMix can be enhanced by adding additional CB in the FE. The reason can be attributed to the decreased internal resistance of the FE. As shown in Fig. 6, R_{int} sharply reduced from 33.7 to 11.8 Ω when 0.75 wt% CB was added to the FE. Increasing the CB amount to 1.0 wt% only resulted in a minor reduction in R_{int}, from 11.8 to 10.7 Ω. The decreased resistance might be attributed to the mesoporous structures of CB. From the N_2 adsorption–desorption experiments (Table 2), both the AC and CB in the present study have a high specific surface area, with a value of 1433.66 and 1405.33 m^2 g^{-1}, respectively. The main difference between these two materials is the pore size distribution (Fig. 8). The AC particles are mainly occupied by micropores with an average pore diameter of 2.14 nm. The microporous

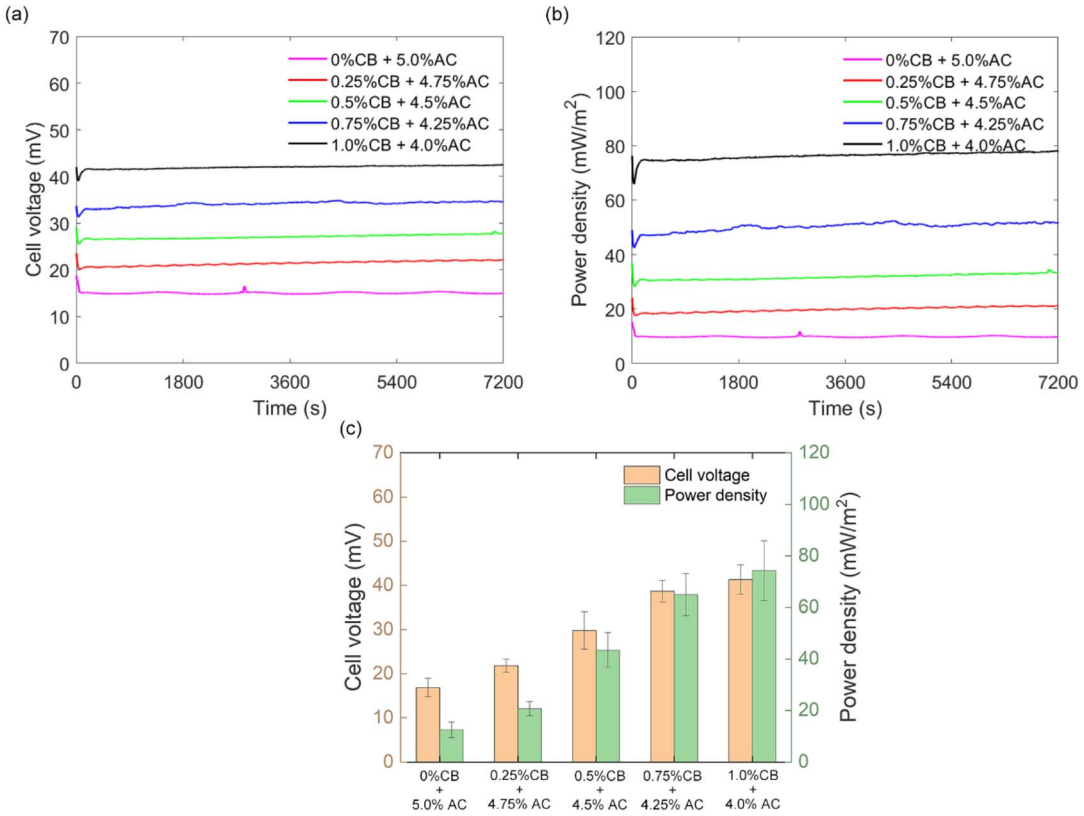

Fig. 5 Plot of (a) the cell voltage and (b) the power density during the experiments of different CB amounts. (c) The average cell voltage and the average power density at different CB amounts, and the error bars denote the standard deviation for the triplicate experiments.

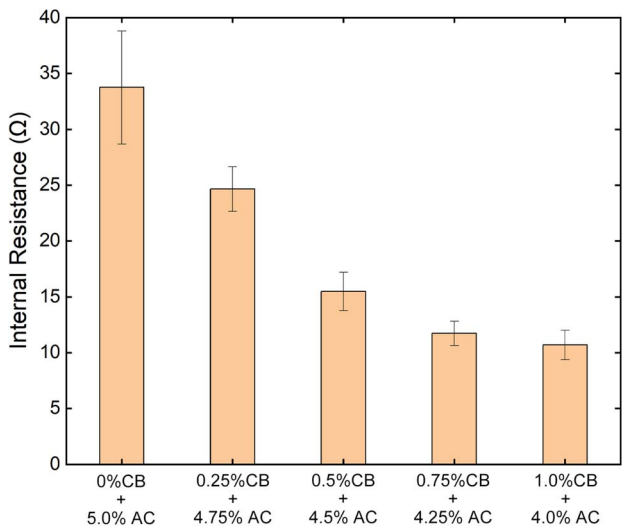

Fig. 6 Plot of cell's internal resistance R_{int} at different carbon black amounts.

structure of AC might result in EDL overlap inside the pores and hinder the ions' transportation.[45] The CB particles, on the other hand, have an average pore diameter of 5.17 nm, which was around 2.4 times larger than that of AC. More importantly, CB is dominated by mesoporous structures with a larger pore size, which might facilitate the ions' transportation and thus reduce the internal resistance.[45] In addition, it should be noted that the performance of the case with 0.75 wt% CB (65 mW m^{-2}) was already greater than that of 10 wt% AC without CB (46 mW m^{-2}). This suggested that only a tiny portion of AC in the FE was able to transport and store the charged ions. Considering that the FE was continuously recirculating between the two graphite plates, the adsorbed ions from the HC were shortly released into the LC. It might be concluded that the charged ions were only stored in the outer part of AC. Therefore, the larger pore size of CB gave a greater system performance even with less AC contents.

3.4 Effect of different types of carbon materials on the system performance

The effect of different types of carbon blacks on the system performance was also investigated in the present study by using

Table 2 The specific surface area (S_{BET}), total pore volume (v_{pore}), micropore volume ($v_{m,pore}$), and average pore size (D_p) of activated carbon (AC) and three different carbon blacks (CB)

	S_{BET} (m^2 g^{-1})	v_{pore} (cm^3 g^{-1})	$v_{m,pore}$ (cm^3 g^{-1})	D_p (nm)
AC	1433.66	0.77	0.63	2.14
CB	1405.33	1.82	0.04	5.17
CB2	805.13	0.93	0.14	4.63
CB3	49.67	0.12	0.01	10.01

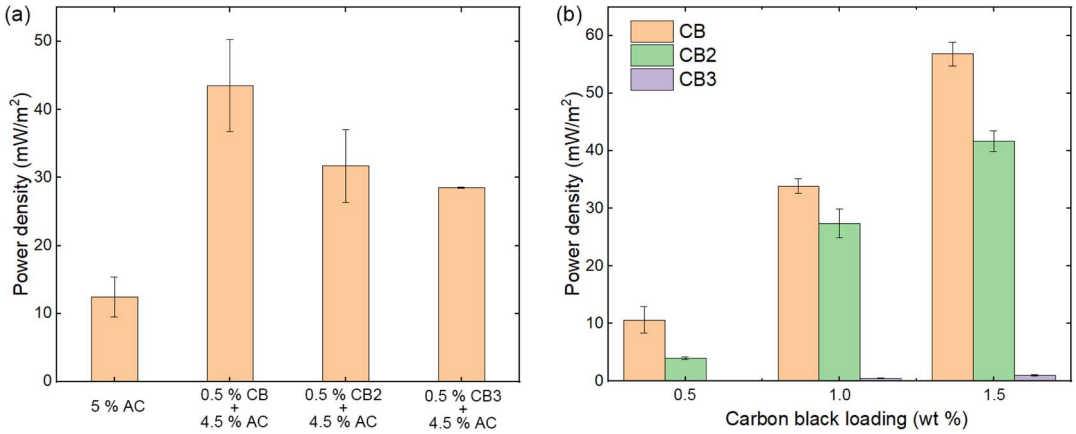

Fig. 7 (a) Power density of F-CapMix under different types of additional carbon black. (b) Power density of F-CapMix by using carbon black as the electrodes. The external resistance is 5 Ω for all the experiments. The error bars denote the standard deviation for the triplicate experiments.

three different types of carbon blacks. As shown in Fig. 7a, all the experimental cases with additional CB produced greater power density compared with the case without CB, which proves again that the additional CB could enhance the system performance. In addition, it has been previously demonstrated that using only CB as the flow electrode could improve the desalination performance.[45] The feasibility of using only CB to produce electricity was experimental examined in the present study. As shown in Fig. 7b, the experimental cases of CB and CB2 produced electricity in both F-CapMix systems, and the power density was proportional to the CB loading, suggesting that it is possible to use these two types of CBs to replace AC as the flow electrode in the F-CapMix system to produce energy. In addition, the power density of using 1.0 wt% amounts of CB and CB2 was greater than the power density of using 5.0 wt% amounts of AC solely, suggesting that these two CBs were more suitable than AC for the energy production of the F-CapMix system. On the other hand, the case of using CB3 produced little electricity in both F-CapMix systems, indicating that CB3 is not suitable as the FE material.

The difference in the system performance under different CB types might be explained by their physical properties. Table 2 shows the N_2 adsorption–desorption experimental results. CB3 has the smallest BET-specific surface area (49.67 $m^2\ g^{-1}$), pore volume (0.12 $cm^3\ g^{-1}$), and micropore volume (0.01 $cm^3\ g^{-1}$) compared to other CBs. Such a low specific surface area and micropore volume of CB3 significantly restricted its ions' storage capacity, thus producing little energy in all the experimental cases (Fig. 7b). By comparing the results of AC with those of CB2, although AC has a higher specific surface area, the power density of AC with 2.5 wt% was lower than that of CB2 with 1.0 wt%, indicating that the specific surface area might not be the only critical factor determining the system performance. By contrast, the pore volume, especially the mesopore volume, seems to be an essential factor for the system performance. The total pore volumes for AC and CB2 are close, at 0.77 and 0.93 $cm^3\ g^{-1}$, respectively. As shown in Fig. 8, AC was mainly occupied by micropores, while CB and CB2 were dominated by mesopores. The mesoporous structure with a larger pore size might facilitate the ions' transportation within the materials

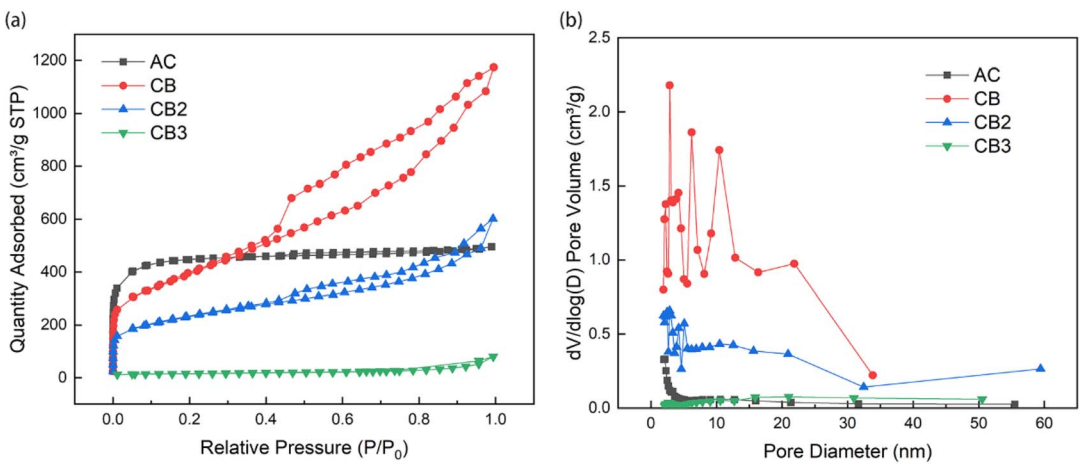

Fig. 8 (a) Nitrogen adsorption isotherms and (b) pore size distribution diagrams of activated carbon (AC) and three different carbon blacks (CB) used in the study.

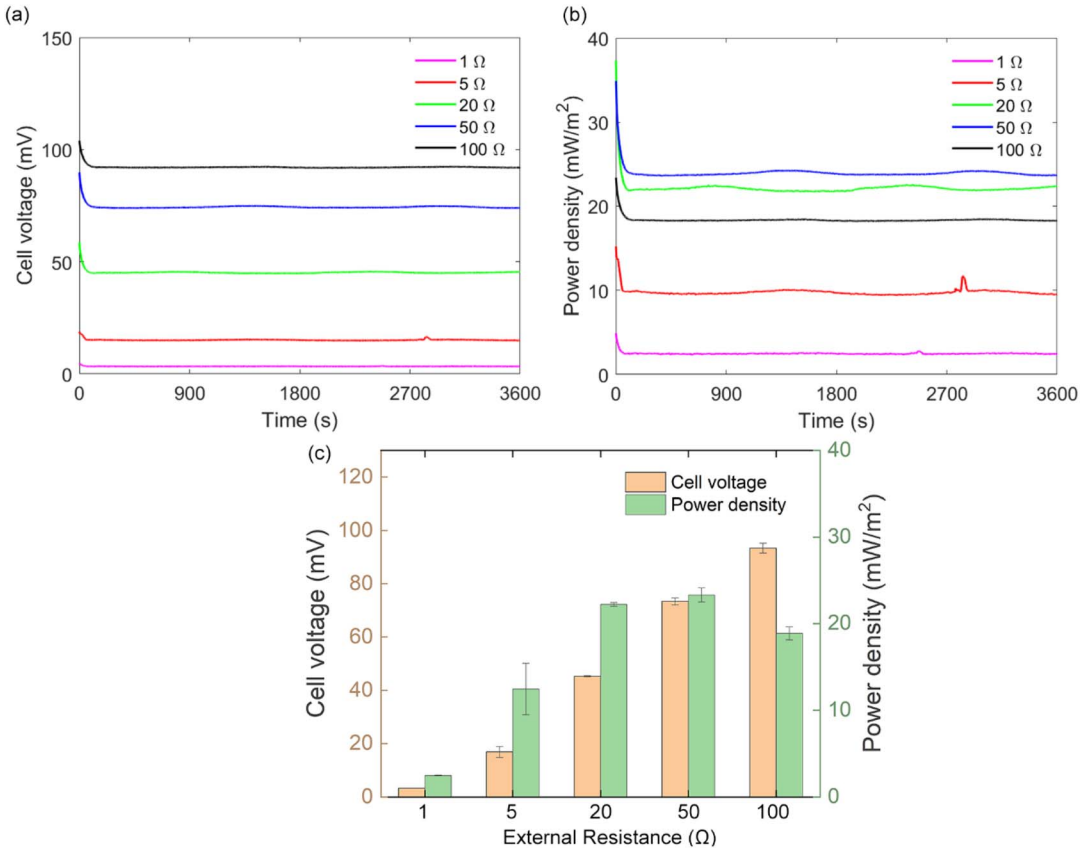

Fig. 9 Plot of (a) the cell voltage and (b) the power density during the experiments of different external resistance. (c) The average cell voltage and the average power density at different external resistances, and the error bars denote the standard deviation for the triplicate experiments.

and enhance the performance.[45,54,55] In addition, the CB and CB2 materials have similar pore sizes and mesoporous structures, but CB with a larger pore volume, which might explain the better system performance when using only CB as the electrodes. Therefore, it might be concluded that a material with a larger specific surface area and mesoporous structure is beneficial for increasing the performance of the F-CapMix system.

3.5 Effect of the external resistance on the system performance

The system performance is dependent on both the cell voltage and the value of external resistance R_{ext} (eqn (2)). In this study, four external resistors (R_{ext} = 1, 20, 50, and 100 Ω) were connected to the cells to investigate the system performance under different resistances. As shown in Fig. 9, the cell voltage V_{cell} was increased with the external resistance R_{ext}. By contrast, the corresponding instantaneous power density P increased with R_{ext} and reached a maximum of 23.3 mW m^{-2} when R_{ext} was 50 Ω. Increasing R_{ext} to 100 Ω led to a 19% reduction in P (18.8 mW m^{-2}). Note that the power density of R_{ext} = 20 Ω (22.2 mW m^{-2}) was very close to the maximum value at R_{ext} = 50 (23.3 mW m^{-2}). It has been suggested previously that the maximum power density can be obtained when the external resistance R_{ext} equals the internal resistance R_{int}.[56,57] Therefore, it might be speculated that R_{int} should be in the middle between 20 and 50 Ω. As can be seen in Fig. 4, the calculated R_{int} was similar for all the cases, at around 33.7 Ω, which explains the similar power density at these two R_{ext}. Meanwhile, the similar R_{int} for all the cases can be explained by the identical FE components (5 wt% AC and 0 wt% CB) of these experiments.

4 Conclusions

In this study, a single-cell F-CapMix system with a cross-chamber configuration has been developed to continuously generate stable electricity from salinity gradient energy between HC and LC solutions for long-term operation. The maximum power density of the system was 74.3 mW m^{-2}, under the experimental conditions of using 4.0 wt% AC loading with additional 1.0 wt% CB under a R_{ext} of 10 Ω. This performance was comparable to those of previous systems of both CapMix with solid electrodes and F-CapMix with flow electrodes. In general, the energy production performance of this single-cell F-CapMix system was dependent on the activated carbon loading, the amount of carbon black, and the external resistance. However, the performance of the single-cell F-CapMix system was independent of the FE electrolyte concentration, which was different from the multiple-cell F-CapMix system.[37] The results suggest that the performance of the system can be enhanced by

increasing either the AC loading or CB amounts due to the reduction in the internal resistance of the system. Furthermore, it is possible to use solely carbon black with a mesoporous structure as the flow electrodes in the F-CapMix system for energy production. In addition, the maximum power density was achieved when the external resistance matched the internal resistance of the system. In summary, these results indicate that the presented single-cell F-CapMix system with a cross-chamber design can produce electricity continuously from the salinity gradient difference between seawater and freshwater.

Author contributions

Zhi Zou: conceptualization, methodology, investigation, writing – original draft, and formal analysis. Shuo Meng: data curation. Xiaolei Bian: data curation. Longcheng Liu: supervision, writing – review, and editing.

Conflicts of interest

There are no conflicts to declare.

Acknowledgements

This work was funded by the Swedish Energy Agency (Energimyndigheten), project number 44606-1. Zhi Zou acknowledges the financial support from the China Scholarship Council (CSC).

References

1 BP, *Statistical review of world energy*, 2021.
2 C. Seyfried, H. Palko and L. Dubbs, *Renewable Sustainable Energy Rev.*, 2019, **102**, 111–120.
3 V. M. Ortiz-Martinez, L. Gomez-Coma, C. Tristan, G. Perez, M. Fallanza, A. Ortiz, R. Ibanez and I. Ortiz, *Desalination*, 2020, **482**, 114389.
4 N. Y. Yip, D. Brogioli, H. V. M. Hamelers and K. Nijmeijer, *Environ. Sci. Technol.*, 2016, **50**, 12072–12094.
5 B. E. Logan and M. Elimelech, *Nature*, 2012, **488**, 313–319.
6 N. Y. Yip and M. Elimelech, *Environ. Sci. Technol.*, 2012, **46**, 5230–5239.
7 R. E. Pattle, *Nature*, 1954, **174**, 660.
8 O. A. Alvarez-Silva, A. F. Osorio and C. Winter, *Renewable Sustainable Energy Rev.*, 2016, **60**, 1387–1395.
9 P. G. Harry, L. Octave and N. Noel de, *Science*, 1974, **185**, 101–102.
10 R. E. Lacey, *Ocean Eng.*, 1980, **7**, 1–47.
11 D. Brogioli, *Phys. Rev. Lett.*, 2009, **103**, 058501.
12 B. B. Sales, M. Saakes, J. W. Post, C. J. N. Buisman, P. M. Biesheuvel and H. V. M. Hamelers, *Environ. Sci. Technol.*, 2010, **44**, 5661–5665.
13 S. Ahualli, M. L. Jimenez, M. M. Fernandez, G. Iglesias, D. Brogioli and A. V. Delgado, *Phys. Chem. Chem. Phys.*, 2014, **16**, 25241–25246.
14 N. Y. Yip, D. A. Vermaas, K. Nijmeijer and M. Elimelech, *Environ. Sci. Technol.*, 2014, **48**, 4925–4936.
15 H. Kim, J. Choi, N. Jeong, H. J. Im, J. G. Yeo, S. I. Jeon, W. G. Chun, D. K. Kim and S. Yang, *ACS Sustainable Chem. Eng.*, 2021, **9**, 9199–9208.
16 G. R. Iglesias, S. Ahualli, A. V. Delgado, P. M. Arenas-Fernandez and M. M. Fernandez, *J. Power Sources*, 2020, **453**, 227840.
17 M. Marino, L. Misuri, M. L. Jimenez, S. Ahualli, O. Kozynchenko, S. Tennison, M. Bryjak and D. Brogioli, *J. Colloid Interface Sci.*, 2014, **436**, 146–153.
18 H. H. Zhu, W. W. Xu, G. C. Tan, E. Whiddon, Y. Wang, C. G. Arges and X. P. Zhu, *Electrochim. Acta*, 2019, **294**, 240–248.
19 G. R. Iglesias, M. M. Fernandez, S. Ahualli, M. L. Jimenez, O. P. Kozynchenko and A. V. Delgado, *J. Power Sources*, 2014, **261**, 371–377.
20 F. Zhan, G. Wang, T. T. Wu, Q. Dong, Y. L. Meng, J. R. Wang, J. Yang, S. F. Li and J. S. Qiu, *J. Mater. Chem. A*, 2017, **5**, 20374–20380.
21 K. Smolinska-Kempisty, A. Siekierka and M. Bryjak, *Desalination*, 2020, **482**, 114384.
22 A. Siekierka, K. Smolinska-Kempisty and M. Bryjak, *Desalination*, 2020, **495**, 114670.
23 B. B. Sales, O. S. Burheim, F. Liu, O. Schaetzle, C. J. N. Buisman and H. V. M. Hamelers, *Environ. Sci. Technol.*, 2012, **46**, 12203–12208.
24 G. R. Iglesias, S. Ahualli, M. M. Fernandez, M. L. Jimenez and A. V. Delgado, *J. Power Sources*, 2016, **318**, 283–290.
25 S. Ahualli, M. M. Fernandez, G. Iglesias, A. V. Delgado and M. L. Jimenez, *Environ. Sci. Technol.*, 2014, **48**, 12378–12385.
26 B. B. Sales, O. S. Burheim, S. Porada, V. Presser, C. J. N. Buisman and H. V. M. Hamelers, *Environ. Sci. Technol. Lett.*, 2014, **1**, 356–360.
27 M. Nasir, Y. Nakanishi, A. Patmonoaji and T. Suekane, *Renewable Energy*, 2020, **155**, 278–285.
28 F. Liu, O. Schaetzle, B. B. Sales, M. Saakes, C. J. N. Buisman and H. V. M. Hamelers, *Energy Environ. Sci.*, 2012, **5**, 8642–8650.
29 M. L. Jimenez, M. M. Fernandez, S. Ahualli, G. Iglesias and A. V. Delgado, *J. Colloid Interface Sci.*, 2013, **402**, 340–349.
30 R. A. Rica, D. Brogioli, R. Ziano, D. Salerno and F. Mantegazza, *J. Phys. Chem. C*, 2012, **116**, 16934–16938.
31 R. A. Rica, R. Ziano, D. Salerno, F. Mantegazza, M. Z. Bazant and D. Brogioli, *Electrochim. Acta*, 2013, **92**, 304–314.
32 D. A. Vermaas, S. Bajracharya, B. B. Sales, M. Saakes, B. Hamelers and K. Nijmeijer, *Energy Environ. Sci.*, 2013, **6**, 643–651.
33 F. Liu, O. Coronell and D. F. Call, *J. Power Sources*, 2017, **355**, 206–210.
34 S. I. Jeon, H. R. Park, J. G. Yeo, S. Yang, C. H. Cho, M. H. Han and D. K. Kim, *Energy Environ. Sci.*, 2013, **6**, 1471–1475.
35 L. Luo, Q. He, Z. X. Ma, D. Yi, Y. Chen and J. X. Ma, *Water Res.*, 2021, **203**, 117522.
36 F. Yang, Y. He, L. Rosentsvit, M. E. Suss, X. Zhang, T. Gao and P. Liang, *Water Res.*, 2021, **200**, 117222.
37 M. C. Hatzell, K. B. Hatzell and B. E. Logan, *Environ. Sci. Technol. Lett.*, 2014, **1**, 474–478.

38 S. Porada, D. Weingarth, H. V. M. Hamelers, M. Bryjak, V. Presser and P. M. Biesheuvel, *J. Mater. Chem. A*, 2014, **2**, 9313–9321.
39 I. Hwang, D. Lee, Y. Jung, K. Park, Y. G. Jung, D. Kim, G. H. Cho, S. I. Jeon, Y. K. Byeun, U. Paik, S. Yang and T. Song, *ACS Sustainable Chem. Eng.*, 2021, **9**, 13514–13525.
40 D. Kim, H. Kwon, G. H. Cho, H. Kim, H. Seo, Y. G. Jung, J. Choi, H. Kim, J. Yoo, D. Lee, I. Hwang, U. Paik, T. Song, H. Park and S. Yang, *Sep. Purif. Technol.*, 2022, **290**, 120859.
41 J. X. Du, P. M. Biesheuvel, W. W. Tang and T. D. Waite, *J. Hazard. Mater.*, 2023, **442**, 130023.
42 W. W. Tang, J. Liang, D. He, J. L. Gong, L. Tang, Z. F. Liu, D. B. Wang and G. M. Zeng, *Water Res.*, 2019, **150**, 225–251.
43 A. Rommerskirchen, A. Kalde, C. J. Linnartz, L. Bongers, G. Linz and M. Wessling, *Carbon*, 2019, **145**, 507–520.
44 W. L. Xing, J. Liang, W. W. Tang, D. He, M. Yan, X. X. Wang, Y. Luo, N. Tang and M. Huang, *Desalination*, 2020, **482**, 114390.
45 J. J. Ma, C. Y. Zhang, F. Yang, X. D. Zhang, M. E. Suss, X. Huang and P. Liang, *Environ. Sci. Technol.*, 2020, **54**, 1177–1185.
46 D. Brogioli, R. Zhao and P. M. Biesheuvel, *Energy Environ. Sci.*, 2011, **4**, 772–777.
47 P. Liang, X. L. Sun, Y. H. Bian, H. L. Zhang, X. F. Yang, Y. Jiang, P. P. Liu and X. Huang, *Desalination*, 2017, **420**, 63–69.
48 K. B. Hatzell, J. Eller, S. L. Morelly, M. H. Tang, N. J. Alvarez and Y. Gogotsi, *Faraday Discuss.*, 2017, **199**, 511–524.
49 F. Yu, Z. Q. Yang, Y. J. Cheng, S. Y. Xing, Y. Y. Wang and J. Ma, *Sep. Purif. Technol.*, 2022, **281**, 119870.
50 H. R. Park, J. Choi, S. Yang, S. J. Kwak, S. I. Jeon, M. H. Han and D. K. Kim, *RSC Adv.*, 2016, **6**, 69720–69727.
51 G. J. Doornbusch, J. E. Dykstra, P. M. Biesheuvel and M. E. Suss, *J. Mater. Chem. A*, 2016, **4**, 3642–3647.
52 K. B. Hatzell, M. C. Hatzell, K. M. Cook, M. Boota, G. M. Housel, A. McBride, E. C. Kumbur and Y. Gogotsi, *Environ. Sci. Technol.*, 2015, **49**, 3040–3047.
53 C. Y. Zhang, J. X. Ma, L. Wu, J. Y. Sun, L. Wang, T. Y. Li and T. D. Waite, *Environ. Sci. Technol.*, 2021, **55**, 4243–4267.
54 M. Tian, Y. Q. Sun, C. Zhang, J. T. Wang, W. M. Qiao, L. C. Ling and D. H. Long, *J. Power Sources*, 2017, **364**, 182–190.
55 L. D. Zou, L. X. Li, H. H. Song and G. Morris, *Water Res.*, 2008, **42**, 2340–2348.
56 S. Cheng, H. Liu and B. E. Logan, *Environ. Sci. Technol.*, 2006, **40**, 2426–2432.
57 T. Kim, M. Rahimi, B. E. Logan and C. A. Gorski, *Environ. Sci. Technol.*, 2016, **50**, 9791–9797.

